

Light Scattering by Marine Particles: Modeling with Non-spherical Shapes

Howard R. Gordon
Department of Physics
University of Miami
Coral Gables, FL 33124

phone: (305) 284-2323 x1 fax: (305) 284-4222 email: hgordon@miami.edu

Grant Number: N000140710226

LONG-TERM GOALS

The long-term scientific goal of my research is to better understand the distribution of phytoplankton in the world's oceans through remote sensing their influence on the optical properties of the water. An associated goal is the understanding of the absorption and backscattering properties of marine particles in terms of the distributions of their size, shape, and composition.

OBJECTIVES

The inherent optical properties (IOPs) of marine particles are most-often modeled as homogeneous spheres using Mie Theory. Although this approach has been fruitful, the next logical step in modeling marine particles is to abandon the normally-employed spherical approximation and use more realistic approximations to their shape. The advent of computer codes capable of handling more complex shapes, and the increased computational speeds now available, suggest that particle modeling employing simple non-spherical shapes, e.g., disks, rods, etc., could become routine. For example, Gordon and Du (2001) used a two-disk model to try to reproduce the backscattering by coccoliths detached from *E. huxleyi* in the blue-green region of the spectrum. They found that the gross morphology of the particle (e.g., modeling the coccolith as parallel disks as opposed to a single disk of the same diameter and volume) was paramount in determining the spectral variation of backscattering. Later Gordon et al. (2009) showed that the resulting spectral variation of the backscattering cross section for the two-disk model agreed with experiment, and that additional fine structure evident in SEM images of coccoliths had only a minor influence on the backscattering. In another study, Clavano et al. (2007) looked at the IOP of spheroids (ellipses of revolution) as a function of their size and aspect ratio (larger major axis divided by smaller major axis) using refractive indices in the range found for marine particles. Their results suggest that, when compared to equal volume spheres, shape can be a significant factor in the IOPs, especially backscattering.

My present work is a continuation of my research into computation of the IOPs of non-spherical objects. Of particular interest to me is the scattering and absorption of particles showing significant deviation from spheres, e.g., cylinders with large aspect ratios or chains of spheres (not necessarily linear). These shapes resemble long chain phytoplankton. How do their scattering and absorption properties depend on the length, diameter and index of refraction of the cylinders or the number, diameter, and index of the individual spheres in a chain? Do their IOPs reach a limit in which they become simply proportional to their length? How do they depend on the distribution of absorbing

Report Documentation Page

*Form Approved
OMB No. 0704-0188*

Public reporting burden for the collection of information is estimated to average 1 hour per response, including the time for reviewing instructions, searching existing data sources, gathering and maintaining the data needed, and completing and reviewing the collection of information. Send comments regarding this burden estimate or any other aspect of this collection of information, including suggestions for reducing this burden, to Washington Headquarters Services, Directorate for Information Operations and Reports, 1215 Jefferson Davis Highway, Suite 1204, Arlington VA 22202-4302. Respondents should be aware that notwithstanding any other provision of law, no person shall be subject to a penalty for failing to comply with a collection of information if it does not display a currently valid OMB control number.

1. REPORT DATE 2009	2. REPORT TYPE	3. DATES COVERED 00-00-2009 to 00-00-2009		
4. TITLE AND SUBTITLE Light Scattering by Marine Particles: Modeling with Non-spherical Shapes			5a. CONTRACT NUMBER	
			5b. GRANT NUMBER	
			5c. PROGRAM ELEMENT NUMBER	
6. AUTHOR(S)			5d. PROJECT NUMBER	
			5e. TASK NUMBER	
			5f. WORK UNIT NUMBER	
7. PERFORMING ORGANIZATION NAME(S) AND ADDRESS(ES) University of Miami, Department of Physics, Coral Gables, FL, 33124			8. PERFORMING ORGANIZATION REPORT NUMBER	
9. SPONSORING/MONITORING AGENCY NAME(S) AND ADDRESS(ES)			10. SPONSOR/MONITOR'S ACRONYM(S)	
			11. SPONSOR/MONITOR'S REPORT NUMBER(S)	
12. DISTRIBUTION/AVAILABILITY STATEMENT Approved for public release; distribution unlimited				
13. SUPPLEMENTARY NOTES				
14. ABSTRACT				
15. SUBJECT TERMS				
16. SECURITY CLASSIFICATION OF:			17. LIMITATION OF ABSTRACT Same as Report (SAR)	18. NUMBER OF PAGES 11
a. REPORT unclassified	b. ABSTRACT unclassified	c. THIS PAGE unclassified		

pigments within the individual links of the chain? How do they depend on orientation? How do they compare to the scattering and absorption by spheres or cylinders containing the same volume of material and absorbing pigment? Is the spherical approximation effective in interpreting their scattering and absorption in terms of an equivalent refractive index? My goal will be to develop an understanding at a level that would allow the incorporation of shape information into IOP models and in the analysis of IOP data.

APPROACH

There are now several computer codes that allow accurate computation of the scattering-absorption properties of individual particles with smooth nonspherical shapes. I have used the discrete-dipole approximation (DDA, Draine, 1988; Draine and Flatau, 1994) in my study of particles similar to *E. huxleyi* coccoliths. I am now using the latest version of the code (DDSCAT 7.0) to study backscattering by randomly oriented finite cylinders with length up to 25 μm and diameters up to 1.5 μm . At this size, an equal volume sphere has a diameter of about 4 μm . Larger particles can be run with the “Amsterdam” DDA (ADDA, Yurkin, et al., 2007), which allows computation of IOPs of particles in a single orientation in a parallel computing architecture; however, orientational averaging with such a code is difficult. In addition, the “generalized multi-particle Mie” method (GMM, Xu and Gustafson, 2001) allows computations of IOPs of clusters of homogeneous and coated spheres (including long chains). Essentially, the GMM method can be used for any problem in which the individual elements (in isolation) can be treated by Mie theory, e.g., coated spheres. Finally, the T-matrix method (Mishchenko et al, 2000) can be used to verify implementation of other codes for simple shapes in cases in which the aspect ratios are not too extreme.

My approach is to use the code that appears most suitable to the computation that is being considered. For example, for a string-of-bead like collection of absorbing spheres the GMM is the obvious choice. I have focused this study on absorbing particles with shapes that are representative of phytoplankton in gross morphology (within the limits of the particular computer code). Comparisons are made between the particle in question and a single homogeneous sphere of equal volume and with the same total concentration of absorbing pigment.

WORK COMPLETED

I have submitted a paper (with T. Smyth, W. Balch and G.C. Boynton) to *Applied Optics* regarding the backscattering by coccoliths detached from *E. huxleyi*. The paper is now in revision. I have completed a study of the scattering and backscattering of non-absorbing cylinders (diameter of 1 μm) as a function of the length and the index of refraction (1.02 to 1.20). The goal was to understand at what aspect ratio (length/diameter) the backscattering becomes essentially proportional to the length. This was mostly carried out using the DDSCAT 6.1 code. For the study of absorbing particles, I have modified the new DDSCAT 7.0 code to include cylinders with interval structure, i.e., a coated cylinder. This is chosen to represent a long chain of phytoplankton, e.g., diatoms, in which the absorbing pigment, if any, is packaged within the internal cylinder. I have completed scattering computations for randomly oriented cylinders (homogeneous and with internal structure, i.e., a coated cylinder) for diameters from 0.5 to 1.5 μm and lengths from 0.5 to a maximum of 15 μm .

A well-known approach to estimating the complex refractive index of marine particles, e.g., phytoplankton, is to measure their extinction and absorption coefficients and the particle volume.

Then the particles are assumed to be spheres and the extinction and absorption efficiencies are computed. Real and imaginary parts of the refractive index are then found, which, for a spherical particle, would yield the same extinction and absorption efficiencies (see for example, Bricaud and Morel, 1986). I have tested this with cylinders ranging in diameter from 0.5 to 1.5 μm and lengths from 0.5 to 15 μm . The two sets of cylinders were homogeneous and had refractive indices 1.05–0.002*i* and 1.05–0.010*i*. Two sets were coated cylinders in which the inner cylinder had a diameter equal to half the cylinder diameter and indices of 1.05–0.008*i* and 1.05–0.040*i*. The outer cladding had an index of 1.05 (no absorption). The cylinder with homogeneous index of 1.05–0.010*i* and the coated cylinder with core index 1.05–0.040*i* have exactly the same quantity (mass) of absorbing pigment. I asked four questions: first, does the way the absorption is distributed within the cylinder (cell) have a significant influence on the IOPs?; second, if the extinction and absorption data are analyzed as described above using the simplified van de Hulst anomalous diffraction theory for the extinction and absorption efficiencies, does the equal-volume sphere with the same extinction and absorption efficiencies yield the correct refractive index?, third, do the retrieved refractive indices yield reasonable approximations to the backscattering in the spherical approximation?, and finally, would better results be obtained using exact scattering theory (Mie) for spheres rather than using the van de Hulst approximation?

RESULTS

While carrying out the study of the scattering and backscattering of non-absorbing cylinders as a function of the length and the index of refraction (1.02 to 1.20), it was found that near a refractive index of 1.05, the DDSCAT 6.1 code produced results that were clearly in error. These computations have been redone using DDSCAT 7.0 and the error does not occur with this version. Figure 1 shows the backscattering coefficient and backscattering probability for a cylinder in random orientation with a diameter of 1 μm , with a refractive index of 1.05, as a function of its length. One would expect that as the cylinder becomes sufficiently long, the backscattering probability should become that of an infinite cylinder. Indeed this is now the case with DDSCAT 7.0. In contrast, DDSCAT 6.1 yielded the nonphysical result of an ever increasing backscattering probability near this refractive index. Figure 2 shows the complete results of the cylinder study for refractive indices from 1.02 to 1.20. Focusing on the red curves, the backscattering probability, one sees that the backscattering probability reaches an asymptotic value near an aspect ratio (length/diameter) of ~ 5 . For cylinders of greater length, the backscattering probability can be estimated from exact computations for infinite cylinders in random orientation.

In the case of absorbing cylinders, we discuss each of the posed questions individually. For the first question (does the way the absorption is distributed within the cylinder (or cell) have a significant influence on the IOPs?), the ratio of the absorption efficiencies Q_a for a coated cylinder with indices $m_{\text{inside}} = 1.05 - 0.040i$ and $m_{\text{outside}} = 1.05 - 0.000i$ ($Q_a(\text{Packaged})$) to that of a homogeneous cylinder $m_{\text{inside}} = m_{\text{outside}} = 1.05 - 0.010i$ ($Q_a(\text{Homo})$) is given in Figure 3. The figure shows that the effect of the absorbing pigment packaging is greatest in the blue region of the spectrum and for larger-diameter cylinders. The maximum decrease in Q_a due to the packaging is about 25%. Although the symbols do not differentiate between cylinder lengths, for a given diameter the packaging effect is largest in the shortest cylinder and depends very little on the length once the aspect ratio (diameter/length) exceeds unity. In the case with less overall absorption, i.e., $m_{\text{inside}} = 1.05 - 0.008i$ and $m_{\text{outside}} = 1.05 - 0.000i$ compared to that of a homogeneous cylinder $m_{\text{inside}} = m_{\text{outside}} = 1.05 - 0.002i$, similar results are obtained; however, the maximum decrease in Q_a due to the packaging is only about 10%.

The van de Hulst anomalous diffraction approximations for the scattering and absorption efficiencies of a homogeneous sphere are,

$$Q_a(\rho') = 1 + 2 \frac{\exp(-\rho')}{\rho'} + 2 \frac{\exp(-\rho') - 1}{\rho'^2}$$

and

$$Q_c(\rho) = 2 - 4 \exp(-\rho \tan \beta) \left[\frac{\cos \beta}{\rho} \sin(\rho - \beta) + \frac{\cos^2 \beta}{\rho^2} \cos(\rho - 2\beta) \right] + 4 \frac{\cos^2 \beta}{\rho^2} \cos(2\beta)$$

where $\rho = 2\alpha(m_r - 1)$, $\rho' = 4\alpha m_i$, and $\tan \beta = m_i/(m_r - 1)$. The combination $m_r - im_i$, is the refractive index of the particle relative to water, and $\alpha = \pi d/\lambda$, with d the sphere's diameter and λ the wavelength of light in the water. Given the volume of the particle (measured for example with a Coulter Counter), and assuming a spherical shape, d and α are determined. Calculations of the beam attenuation coefficient and absorption coefficients for coated cylinders were inserted in these equations to find m_r and m_i . Figure 4 provides the resulting computations for a coated cylinder with indices $m_{inside} = 1.05 - 0.040i$ and $m_{outside} = 1.05 - 0.000i$, and all combinations of diameter and length. Ideally one should derive an index of $1.05 - 0.010i$, based on the concentration of absorbing material. Clearly, m_i is retrieved to within $\pm 20\%$ with an average (over all sizes) close to 0.010, and the retrieved m_r appears to be too low in all cases, but averages ~ 1.044 . I am still carrying out the analysis of these computations, but it is clear that applying the above formulas to scattering data yields meaningful results even for particles with large aspect ratios.

In regard to the backscattering computed using the retrieved refractive indices and the size, Figure 5 provides one example for a refractive indices of $m_{inside} = 1.05 - 0.010i$ and $m_{outside} = 1.05 - 0.010i$, i.e., a homogeneous cylinder. One notes that for the large aspect ratio (AR = cylinder length divided by diameter), the computed backscattering is too low by as much as a factor of 7, while in contrast, for low aspect ratios the computed backscattering is within $\sim 20\%$ of the true value. Thus as noted before, e.g., see Clavano et al (2007), the backscattering by high aspect ratio particles is much larger than that of an equivalent volume sphere.

As for the final question (i.e., would better results be obtained using exact scattering theory (Mie) for spheres instead of the analytical van de Hulst approximation?), I have only examined a small number of cases by trial and error. These cases suggest that there is little difference between using the van de Hulst approximation and using the exact Mie theory. However, for particles of higher refractive index, this may not be the case.

IMPACT/APPLICATIONS

The fact that backscattering probability by cylinders with aspect ratios of 5-10 becomes independent of the aspect ratio, and hence backscattering becomes proportional to the length, can be used to simplify computations for long cylinders. It also suggests that the rigorous EM scattering from infinite cylinders can be used to estimate backscattering probability of finite cylinders. Although a full analysis remains to be completed, the study of absorbing cylinders suggests that the methods used by other investigators to estimate the refractive index of, for example phytoplankton, is capable of yielding reasonably accurate results even for high-aspect ratio inhomogeneous cylinders.

REFERENCES

Bricaud, A. and A. Morel, Light attenuation and scattering by phytoplanktonic cells: a theoretical modeling, *Applied Optics*, **25**, 571—580 (1986).

Calvano, W. R., E. Boss, and L. Karp-Boss, Inherent Optical Properties of Non-spherical Marine-Like Particles – From Theory to Observation., *Oceanography and Marine Biology: An Annual Review*, **45**, 1—38 (2007).

Draine, B.T., The discrete-dipole approximation and its application to interstellar graphite grains. *Astrophys. J.* **333**: 848–872, 1988.

Draine, B.T. and P. Flatau, "Discrete-dipole approximation for scattering calculations," *J. Opt. Soc. Am. A* **11**, 1491–1499, 1994.

Gordon, H.R. and Tao Du, Light scattering by nonspherical particles: application to coccoliths detached from *Emiliania huxleyi*, *Limnology and Oceanography*, **46**, 1438–1454, 2001.

Gordon, H.R., T.J. Smyth, W.M. Balch, and G.C. Boynton, Light scattering by coccoliths detached from *Emiliania huxleyi*, *Applied Optics*, (2009).

van de Hulst, H.C., 1957. *Light Scattering by Small Particles*, Wiley.

Xu, Yu-lin, and Bo A.S. Gustafson, A generalized multiparticle Mie-solution: further experimental verification, *Journal of Quantitative Spectroscopy & Radiative Transfer* **70** 395–419, 2001.

Yurkin, M. A., K. A. Semyanov, V. P. Maltsev, and A. G. Hoekstra, 2007, Discrimination of granulocyte subtypes from light scattering: theoretical analysis using a granulated sphere model, *Opt. Express* **15**, 16561–16580.

PUBLICATIONS

C.P.Kuchinke, H.R. Gordon, and B.A. Franz, Spectral optimization for constituent retrieval in Case 2 waters I: Implementation and performance, *Remote Sensing of Environment*, **113**, 571—587, 2009. (doi:10.1016/j.rse.2008.11.001). [published, refereed]

C.P. Kuchinke, H.R. Gordon, L.W. Harding, Jr., and K.J. Voss, Spectral optimization for constituent retrieval in Case 2 waters II: Validation study in the Chesapeake Bay, *Remote Sensing of Environment*, **113**, 610—621, 2009. (doi:10.1016/j.rse.2008.11.002). [published, refereed]

H.R. Gordon, Estimation of space-borne lidar return from natural waters: A passive approach, *Optics Express*, **17(6)**, 4677—4684 (2009). [published, refereed]

H.R. Gordon, M.R. Lewis, S.D. McLean, M.S. Twardowski, S.A. Freeman, K.J. Voss, and G.C. Boynton, Spectra of particulate backscattering in natural waters, *Optics Express*, **17**, 16192—16208 (2009). [published, refereed]

V.F. Banzon, H.R. Gordon, C.P. Kuchinke, D. Antoine^c, K.J. Voss, and R.H. Evans, Validation of a SeaWiFS dust-correction methodology in the Mediterranean Sea: identification of an algorithm switching criterion, *Remote Sensing of Environment*, (2009). [refereed, in press]

H.R. Gordon, T.J. Smyth, W.M. Balch, and G.C. Boynton, Light scattering by coccoliths detached from *Emiliania huxleyi*, *Applied Optics*, (2009). [submitted, in revision]

$$m = 1.05$$

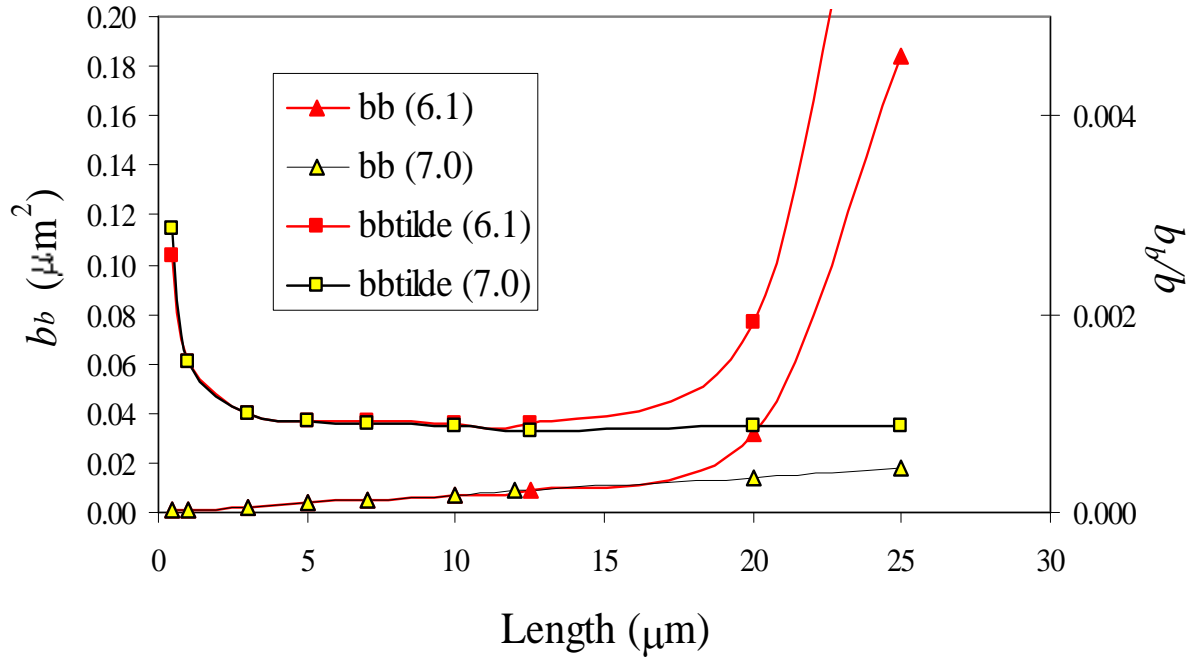


Figure 1. The backscattering cross section (“bb,” triangular symbols, left “y”-axis) and the backscattering probability (“bbtilde,” square symbols, right “y”-axis) for a right circular cylinder with a diameter of 1 \$\mu\text{m}\$, and a refractive index of 1.05, as a function of its length. The cylinder orientation is random. The computations are carried out with DDSCAT 6.1 (red symbols) and 7.0 (yellow filled symbols with a black border). Note that in the case of 7.0, the backscattering probability reaches an essential constant value of \$\sim 0.00086\$ near a length of \$\sim 5 \mu\text{m}\$ (aspect ratio of 5), while the 6.1 computation shows an ever increasing backscattering probability for lengths greater than 15 \$\mu\text{m}\$.

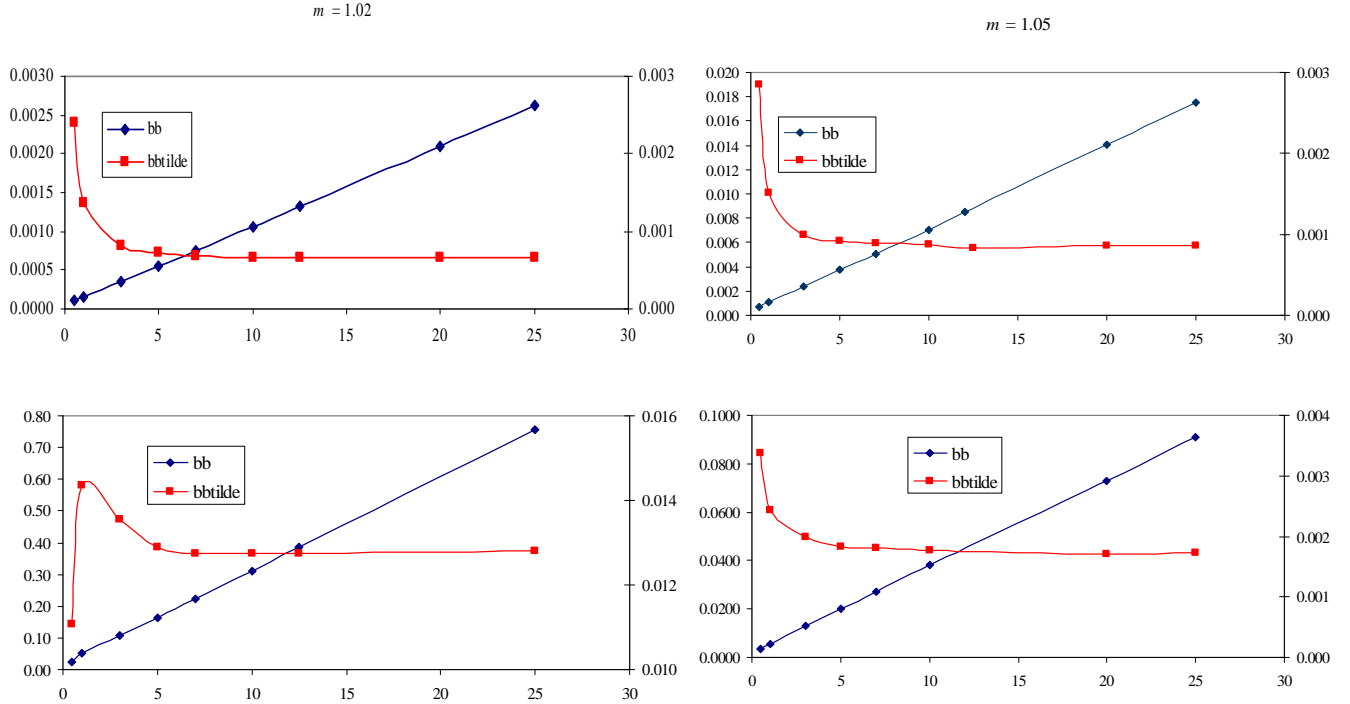


Figure 2 . These figures provide the backscattering cross section (“bb,” blue curves, left “y”-axis in μm^2) and the backscattering probability (“bbtilde,” red curves, right “y”-axis) for a right circular cylinder with a diameter of 1 μm as a function of its length (“x”-axis) in μm . The individual panels are for refractive indices (clockwise from the upper left) of 1.02, 1.05, 1.10, and 1.20. For all of the refractive indices, the backscattering probability becomes essentially constant for aspect ratios greater than 5 to 10.

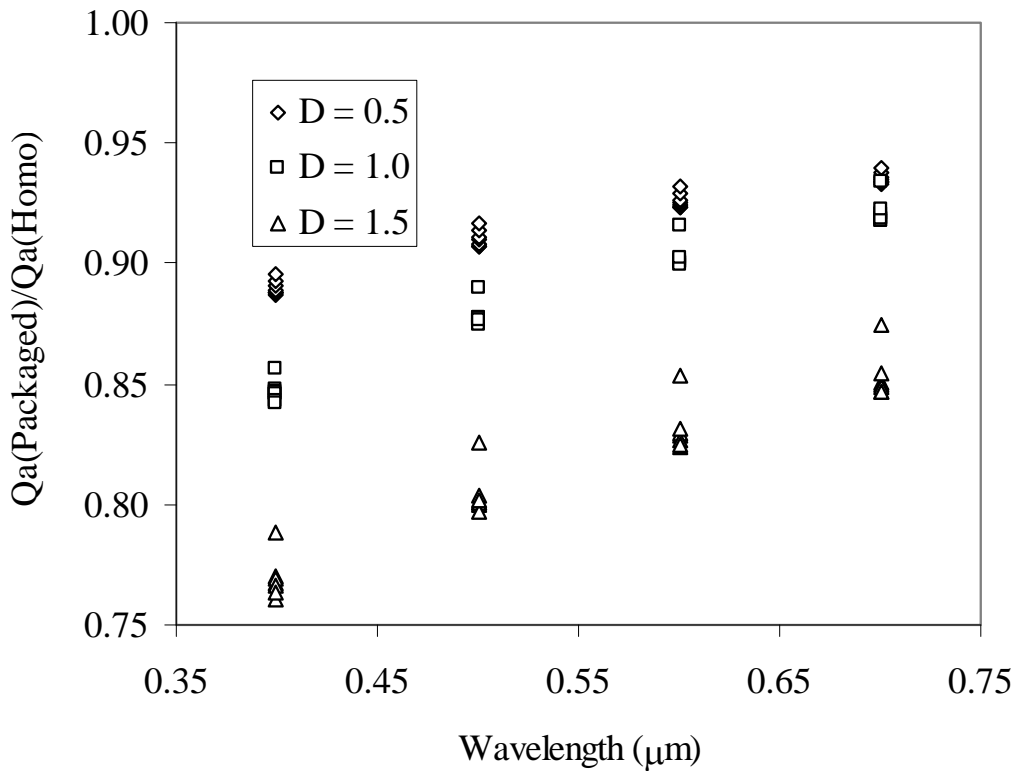


Figure 3. This figure provides the ratio of absorption efficiencies (coated to homogeneous) of strongly absorbing cylinders as a function of wavelength. The diameter of the cylinder (in μm) is specified in the legend. For each diameter, the symbols refer to cylinder lengths ranging from 0.5 to 15 μm . The figure shows that the effect of the absorbing pigment packaging is greatest in the blue region of the spectrum and for larger-diameter cylinders. Although the symbols do not differentiate between cylinder lengths, for a given diameter the packaging effect is smallest in the shortest cylinder and depends very little on the length once the aspect ratio (length/diameter) exceeds unity.

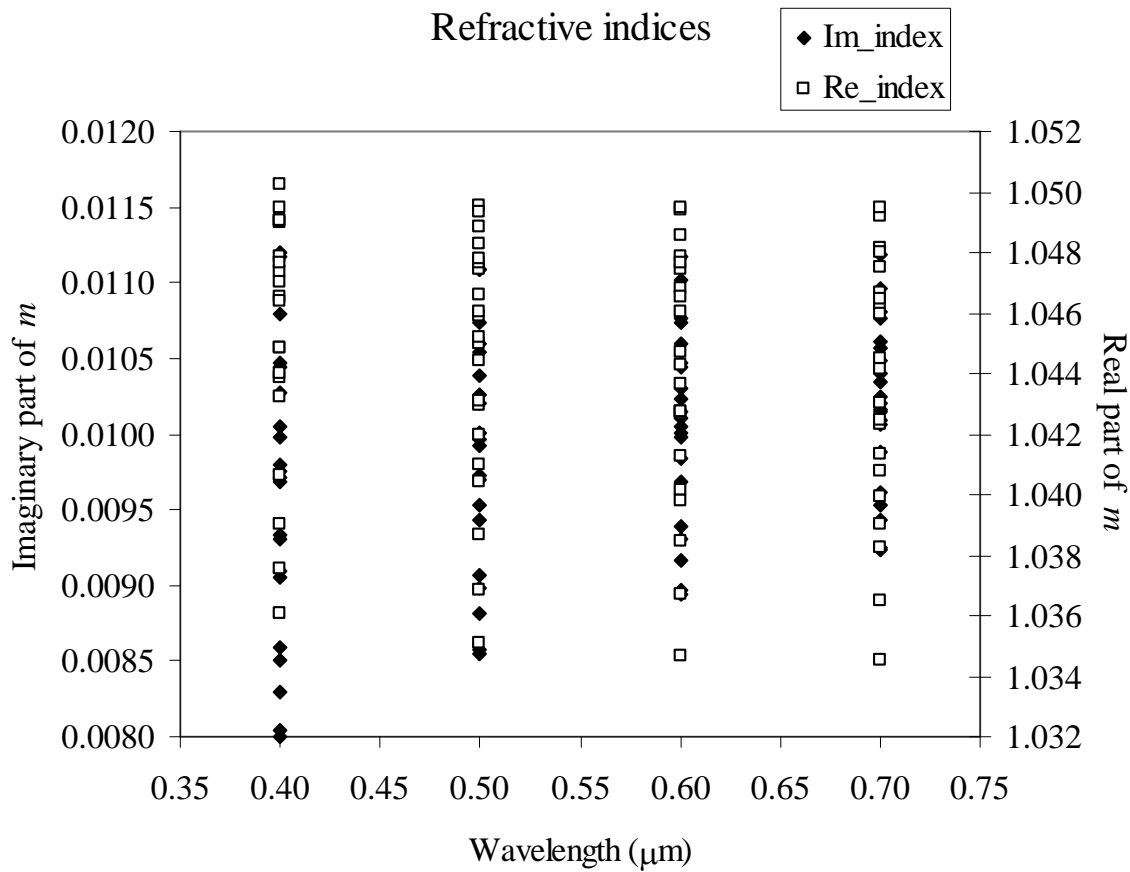


Figure 4. An example of retrievals of the real and imaginary parts of the refractive index for coated cylinders for all the combinations of diameter and length, using the van de Hulst approximation. Ideally one should derive a real part of 1.05 and an imaginary part of 0.010. The scatter shows that m_i is retrieved to within $\pm 20\%$ (somewhat better in the red) with an average (over all sizes) close to 0.010, and that the retrieved m_r appears to be too low in almost all cases, but averages ~ 1.044 .

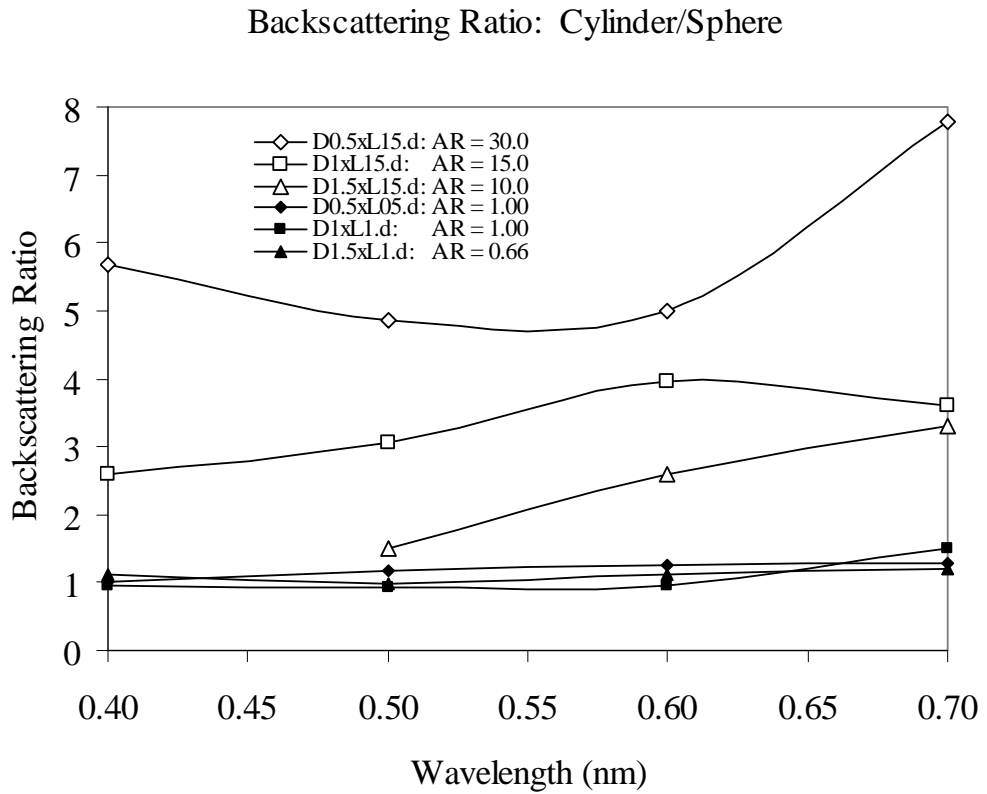


Figure 5: The ratio of backscattering (Cylinder \div Sphere) for cylinders with high and low aspect ratios “AR”. In the legend, the code “D0.5xL15.d” indicates that the diameter of the cylinder is 0.5 m and the length is 15 m, etc. The graph shows that the backscattering by high-aspect ratio cylinders is much greater than that of equal volume spheres, while cylinders with aspect ratio near unity backscatter in a manner similar to spheres.